Korean Journal of Chemical Engineering (2024) 41:2287–2296
https://doi.org/10.1007/s11814-024-00184-4

ORIGINAL ARTICLE

Preparation of Sulfonated Cross-Linked Films for Proton Exchange Membranes (PEMs) Through a Curing Process

Suk-Yong Jang[1] · Ji-Su Lee[1] · Seung-Gi Oh[1] · Sien-Ho Han[1]

Received: 6 December 2023 / Revised: 24 April 2024 / Accepted: 26 April 2024 / Published online: 21 June 2024

Abstract

Raw-poly(*n*-butyl acrylate (BA)-sodium styrene sulfonate (SS)-neopentyl glycol diacrylate (NPGDA)) (raw-PBSN) films were prepared through a curing process from various BA/SS/NPGDA mixtures (BSN mixture). Sulfonation of the raw-PBSN films was performed via a pretreatment process. As a result, light-brown sulfonated PBSN (SPBSN) films with a thickness of 80 ~ 95 μm were obtained. The ion exchange capacity (IEC), proton conductivity (PC), swelling ratio (SR), and water uptake (WU) of these specimens were improved with an increase in the content of SS within the SPBSN matrix. The SPBSN 25 wt%, SPBSN 30 wt% and SPBSN 35 wt% films containing corresponding SS contents of 25 wt%, 30 wt% and 35 wt%, which are much higher IEC values compared to that of Nafion® 117. Specifically, the PC value of the SPBSN 35 wt% film was approximately 0.211 S/cm, nearly 22.6% higher than that of Nafion® 117 (0.172 S/cm) at a temperature of 80 °C and relative humidity (RH) of 100%. A fourier transform infrared spectroscopy (FT-IR) analysis was conducted to verify the sulfonation of the raw-PBSN films. A transmission electron microscope (TEM) analysis served to investigate the hydrophilic domain images of the SPBSN films.

Keywords PEFCs · Sulfonation · Pretreatment · Cross linking · SPBSN

Introduction

Since the initial report of the fuel cell by Sir William R. Grove in 1839, polymer electrolyte fuel cells (PEFCs) have been attracting a considerable amount of attention as a clean energy source for transportation and stationary applications [1, 2]. Nevertheless, the major factor hindering the widespread commercial adoption of PEFCs is the high cost of perfluorinated PEMs (Nafion®) [3]. Therefore, many researchers have studied the development of inexpensive non-perfluorinated PEMs, such as sulfonated poly(ether ether ketone) (SPEEK) [4], sulfonated polybenzimidazole (SPBI) [5], sulfonated poly(arylene ether) (SPAE) [6], sulfonated polyimide (SPI) [7], sulfonated poly(styrene ethylene butylene styrene) (SSEBS) [8] and others. These studies fundamentally focused on the sulfonation of a styrene-based linear polymer or styrene-based copolymers dissolved in organic solvents [9]. Sulfonated styrene-based cross-linked polymers as PEMs in PEFCs may be preferred due to their excellent mechanical and chemical properties. However, because these types of polymers are insoluble in organic solvents, they cannot be applied in this capacity [10]. To overcome these drawbacks, Sato et al. reported, in a research paper entitled "synthesis of a cross-linked polymer electrolyte membrane with an ultra-high density of sulfonic acid groups," the use of a conventional synthetic method (radical copolymerization method). Their study found that the PC value of a cross-linked poly(styrene-sulfonic acid) (CL-sSA) film at 80 °C and 90% HR was 0.093 S/cm [11]. Sun et al. also found that the PC value of a cross-linked PSSNa-PVDF-OX film based on poly(sodium 4-styrene sulfonate) (PSSNa) and poly(vinylidene fluoride (PVDF) combined with the additive oxalic acid (OX) and processed using a slurry-casting approach reached 0.050 S/cm at 80 °C and 95% RH [12]. Kim et al. investigated cross-linked poly(styrene-NaSS-UAN) random copolymers (PSSU) consisting of a sulfonated monomer (NaSS) and a non-sulfonated monomer (styrene) through a radical copolymerization method. Their highest PC value was 0.10 S/cm at 60 °C and 95% RH [13]. Despite the many efforts listed above, sulfonated

✉ Sien-Ho Han
han@tukorea.ac.kr

[1] Department of Chemicial Engineering and Biotechnology, Tech University of Korea, 237 Sangidaehak-Ro, Siheung-Si, Gyeonggi-Do 15073, Republic of Korea

styrene-based cross-linked polymer films as PEMs have much lower PC and IEC values compared to those of sulfonated styrene-based linear polymer and sulfonated styrene-based copolymer films.

Our laboratory utilized BA, SS and NPGDA monomers containing one and two carbon–carbon double bonds at the main chain given that a functional monomer can easily cross-link independently [14, 15]. Raw-PBSN films in the sodium salt form were cross-linked through free radical reactions between their reactive vinyl segments in BSN mixtures [12, 16]. SPBSN films were prepared by substituting –Na with –H at the phenyl side chains of the SS that exists in the raw-PBSN films without a dissolving process in an organic solvent [11, 17]. Interestingly, the IEC values of the SPBSN 25 wt%, SPBSN 30 wt% and SPBSN 35 wt% films were approximately 3.42 meq/g, 4.48 meq/g and 5.12 meq/g, respectively, close to 93.2%, 153.1% and 189.2% higher compared to that of Nafion® 117 (1.77 meq/g) under identical conditions. The corresponding PC values of the SPBSN 30 wt% and 35 wt% films were approximately 0.179 S/cm and 0.211 S/cm, close to 4.0% and 22.6% higher compared to that of Nafion® 117 at 80 °C and 100% RH. The purpose of this study is to present a new method by which to prepare sulfonated cross-linked films for PEFCs using various functional monomers through a curing process. Another goal is to investigate the SR, WU, IEC and PC characteristics and to capture TEM images of each film sample with different contents of SS within the SPBSN matrix.

Experimental

Materials

BA, SS, NPGDA, 2,20-azobisiso-butyronitrile (AIBN) and dimethyl sulfoxide (DMSO) were purchased from Sigma Aldrich & Merck and were used as received.

Preparation of the Raw-PBSN and SPBSN Films

First, the BA, SS, and NPGDA monomers were dissolved in DMSO to form homogeneous BSN mixtures with different contents of sodium salt groups [14, 15]. Then, a radical initiator, AIBN, in this case, was added to the BSN mixtures. Subsequently, the BSN mixtures were poured into a silicone-packed mold (silicone rubber thickness: 0.1 mm) and then cured for polymerization at 70 °C for 30 min [15, 18]. Raw-PBSN films with a thickness of 85 ~ 95 µm were thus obtained. In order to remove the unreacted monomers, the raw-PBSN films were immersed in a water–acetone (1:1 mix ratio) solution for 12 h [11, 19]. These films were also immersed in an 80 °C peroxide (H_2O_2) solution of 10% for 1 h to remove residual impurities [12, 20]. Finally, the films were acidified into the sulfonated film form by immersion in an 85 °C sulfuric acid (H_2SO_4) solution of 0.5 M for 3 h. Figure 1 shows the chemical structure of the SPBSN films and Fig. 2 shows the corresponding preparation process. Figure 3 shows photographs of both dried and hydrated SPBSN films. The materials used for the preparation of the SPBSN films are summarized in Table 1.

FT-IR Measurement

The FT-IR spectra were recorded in transmittance mode on a Fourier-transform infrared spectrophotometer (FT-IR, Perkin Elmer Spectrum One) in a wave number range from 500 to 4000 cm^{-1}.

Oxidative Stability Measurement

The oxidative stability was determined by immersing a small specimen of film (size: 1.0 × 1.0 cm) into a 3% H_2O_2 aqueous solution containing 4 ppm $FeCl_2 \bullet 4H_2O$ at 80 °C for up to 240 h. The specimens were cleaned with deionized water several times and then dried at 120 °C. Degradation of the SPBSN films was measured according to the weight loss.

Thermogravimetric Analysis Measurement

The thermogravimetric analysis (TGA) was conducted using Trios v5.1.1.46572 (TA Instruments, New Castle, DE, USA) from 25 to 500 °C at 5 °C/min in nitrogen gas flushed at 150 ml/min.

Swelling-Ratio Measurement

The SR of PEMs is an important factor influencing the PC, IEC, mechanical and chemical properties, and stability and durability of PEMs in PEFCs. It is known that a proton (H^+) can be transferred along with hydrophilic domains such as H_3O^+, $H_5O_2^+$and $H_9O_4^+$, as the water existing in PEMs serves as a conducting medium for H^+. However, excessive water in PEMs can cause morphologic changes to the membrane. The SR level in this study was determined by measuring the variation in the thickness between wet and dry SPBSN film specimens (size: 1.0 × 1.0 cm). The dry SPBSN film was immersed in deionized water at room temperature for 24 h. The SR level of the SPBSN films was calculated by the following equation [21, 22]:

$$SR(\%) = \frac{S_{wet} \times S_{dry}}{S_{dry}} \times 100,$$

where S_{wet} and S_{dry} represent the thickness of the swollen and dried film, respectively.

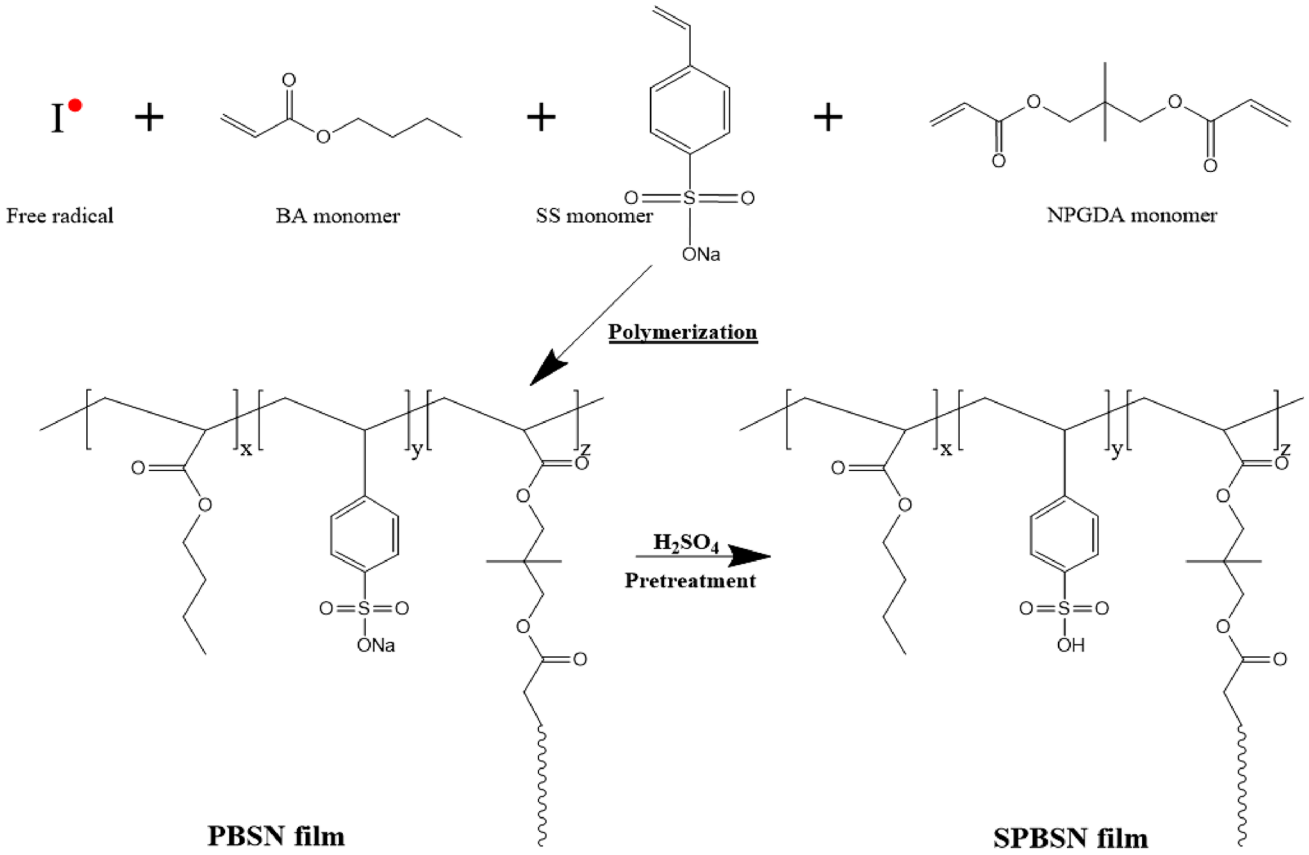

Fig. 1 Chemical structure of the SPBSN films

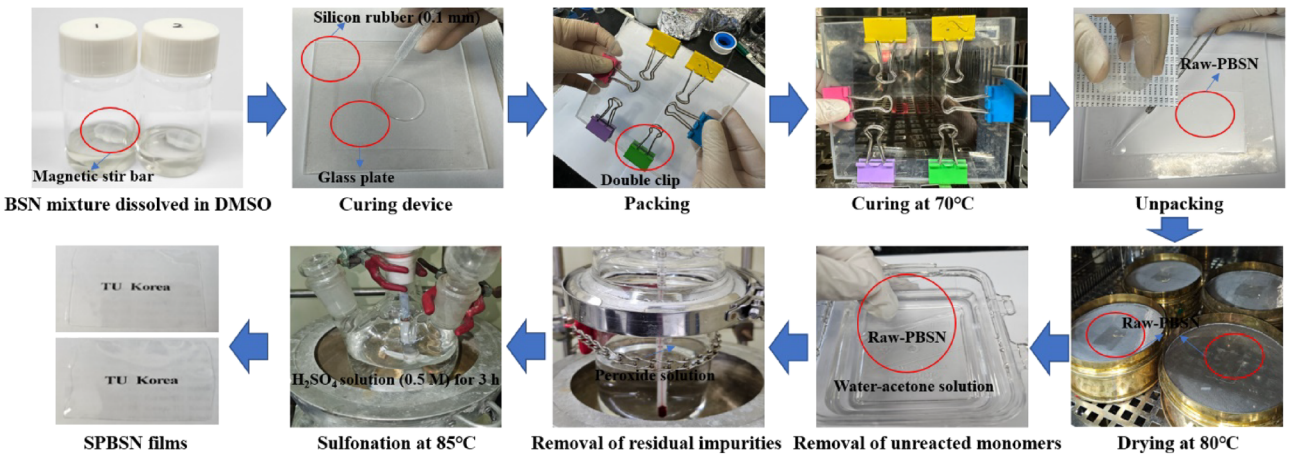

Fig. 2 Preparation process of the SPBSN films

Water Uptake Measurement

With regard to the WU measurements, the evaluation process is similar to that used for the swelling-ratio measurements.

The WU level of the SPBSN films was calculated by the following equation [22]:

$$WU(\%) = \frac{W_{\text{wet}} \times W_{\text{dry}}}{W_{\text{dry}}} \times 100,$$

where W_{wet} and W_{dry} represent the weights of the swollen and dried film, respectively.

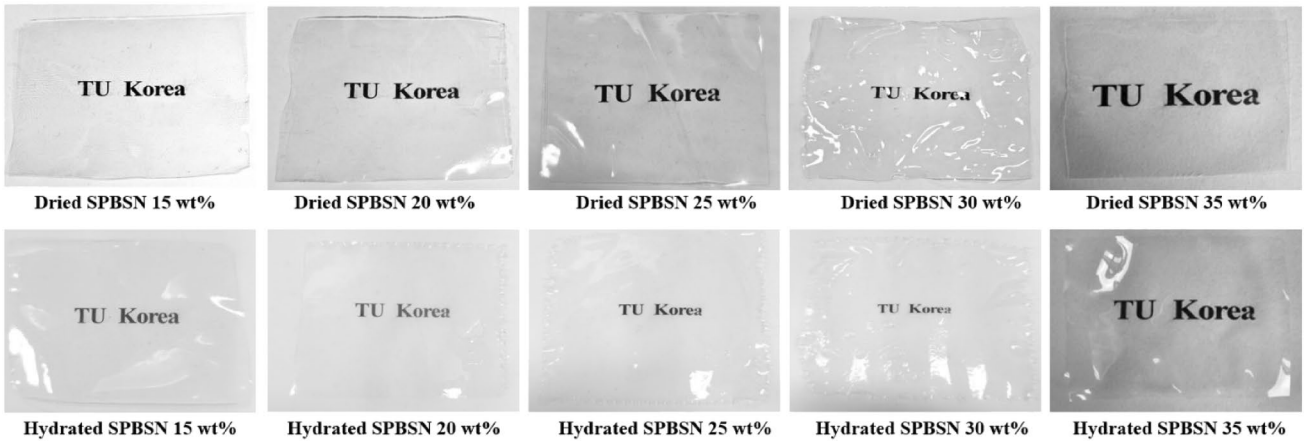

Fig. 3 Photographs of the dried and hydrated SPBSN films

Table 1 Preparation recipes of the SPBSN films

Sample	BA	SS	NPGDA	DMSO	AIBN	Curing	Pretreatment
Nafion® 117	–	–	–	–	–	No	Yes
SPBSN 15 wt%	0.0039 mole (0.50 g)	0.0008 mole (0.17 g (15 wt%))	0.0023 mole (0.50 g)	2.50 g	0.01 g	Yes	Yes
SPBSN 20 wt%	0.0039 mole (0.50 g)	0.0012 mole (0.25 g (20 wt%))	0.0023 mole (0.50 g)	2.50 g	0.01 g	Yes	Yes
SPBSN 25 wt%	0.0039 mole (0.50 g)	0.0016 mole (0.33 g (25 wt%))	0.0023 mole (0.50 g)	2.50 g	0.01 g	Yes	Yes
SPBSN 30 wt%	0.0039 mole (0.50 g)	0.0020 mole (0.43 g (30 wt%))	0.0023 mole (0.50 g)	2.50 g	0.01 g	Yes	Yes
SPBSN 35 wt%	0.0039 mole (0.50 g)	0.0026 mole (0.54 g (35 wt%))	0.0023 mole (0.50 g)	2.50 g	0.01 g	Yes	Yes

Ion Exchange Capacity Measurement

The IEC of PEMs is a critical factor when predicting the PC value. IEC value in this study was measured through the titration of the amount of H^+ released from a pre-weighed film in a sulfonated form using 1 M sodium chloride (NaCl) with 0.01 M sodium hydroxide (NaOH) and phenolphthalein. The IEC value was obtained as the average of each film in units of the milli-equivalents NaOH per gram of the SPBSN film and was calculated with the following equation [23, 24]:

$$\mathrm{IEC} = \frac{N_{\mathrm{NaOH}} \times V_{\mathrm{NaOH}}}{W_{\mathrm{dry}}} \times 100\%,$$

where N_{NaOH}, V_{NaOH} and W_{dry} are the concentration, the consumed volume of NaOH and the weight of the dried SPBSN film, respectively.

Proton-Conductivity Measurement

The PC value of the SPBSN films (size: 1.0 × 1.0 cm) can be calculated by the following equation [25, 26]:

$$\sigma = \frac{L}{RWD}.$$

Here, σ is the PC (S/cm), L is the distance between the electrodes for the voltage measurement (cm), R is the resistance (Ω), W is the effective film surface area (cm) and D is the film thickness (cm). In addition, R was measured by alternative resistance (ac) impedance spectroscopy using an electrode system connected to an impedance/gain-phase analyzer and an electrochemical interface (SP-150, Bio-Logic Instruments, France). The PC value of the SPBSN films was measured at constant humidity rates (over 95% relative humidity) and temperatures (50, 60, 70 and 80 °C).

Morphology Measurement

The morphologies of the Nafion® 117 and SPBSN films were confirmed by transmission electron microscopy (TEM, JEM-2100F, JEOL).

Results and Discussion

FT-IR of the SPBSN Films

Figure 4 shows the FT-IR spectra of the BA monomer, NPGDA monomer and poly(BA-NPGDA) (PBN) copolymer. As shown in Fig. 4, the acrylate peak (C = C) of the BA and NPGDA monomer is observed at 1636 cm^{-1} [25]. The acrylate peak of the PBN copolymer has completely vanished. Because functional monomers can extend a chain through reactions between their acrylic groups [5.7], these FT-IR results show that cross-linking polymerization was suitably performed via the curing process.

Figure 5 shows the FT-IR spectra of the SPBSN film specimens. The typical peaks of the sulfonic acid group, SO_3H, are observed at 600 ~ 700 cm^{-1}, 1030 ~ 1060 cm^{-1} and 1150 ~ 1250 cm^{-1} [25, 26]. The SPBSN films exhibit characteristic peaks at 1030 cm^{-1} and 1060 cm^{-1}, attributable to the asymmetric and symmetric stretching vibration of the sulfonic acid group of $–SO_3$, respectively [27]. The absorption band centered at 600 cm^{-1} and 690 cm^{-1} is ascribed to the S–O of the sulfonic acid group [21]. These FT-IR results indicate that the PBSN films were successfully sulfonated via the pretreatment process.

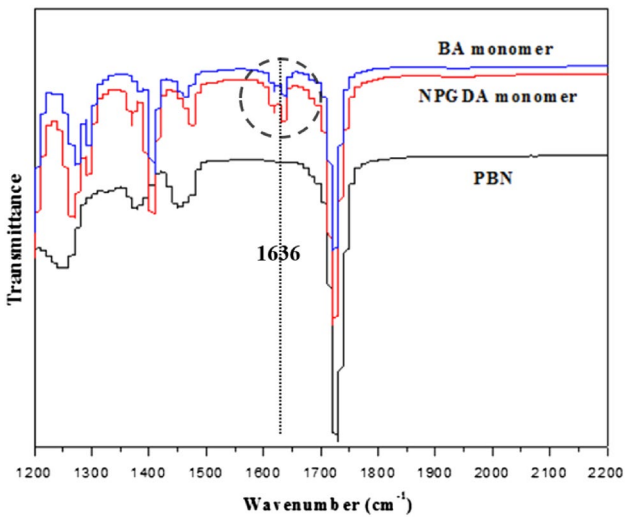

Fig. 4 FT-IR spectra of the BA, NPGDA monomers and PBN copolymer

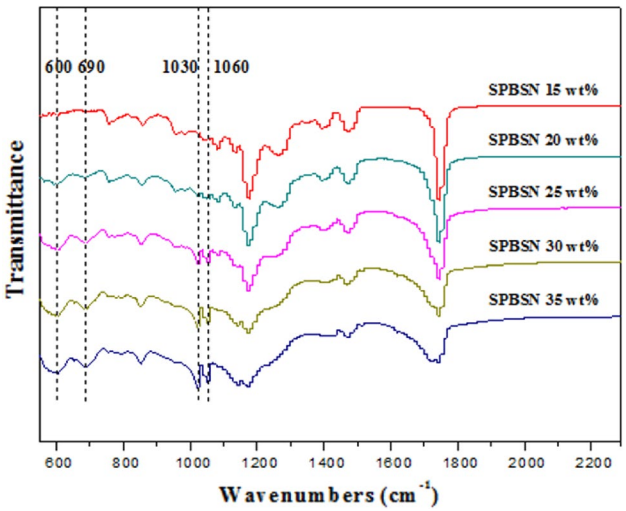

Fig. 5 FT-IR spectra of the SPBSN films

Purification of the SPBSN Films

Figure 6 shows the unreacted monomer content of the SPBSN films. As shown in this figure, the unreacted monomer content increased with an increase in the concentration of the sulfonic acid group in the SPBSN matrix. In particular, the unreacted monomer content of the SPBSN 35 wt% specimen is approximately 9.59%, nearly 2.5 times higher compared to that of the SPBSN 15 wt% specimen (approximately 3.76%). We expect that the excessive SS content played a role in interrupting the radical polymerization and decreasing the compatibility in the BSN mixtures [13, 14]. The unreacted monomer content of the SPBSN films was calculated using the WU and SR equations mentioned above.

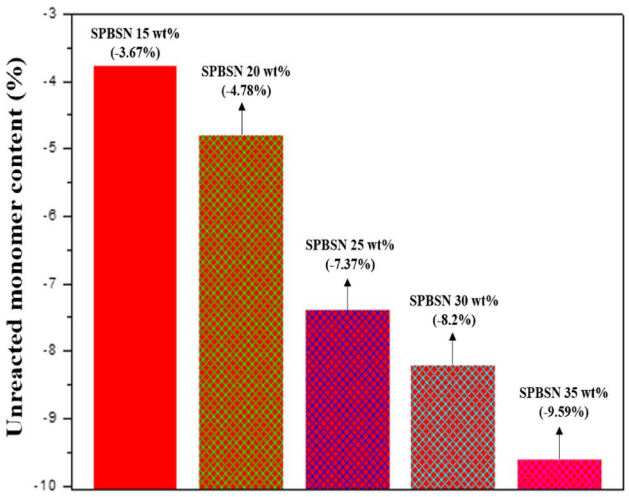

Fig. 6 Purification of the SPBSN films

Oxidative Stability of the SPBSN Films

Figure 7 shows the chemical stability of the SPBSN films. As shown in this figure, the weight loss increased with an increase in the concentration of the sulfonic acid group in the SPBSN matrix. Two distinct weight loss steps were observed for all SPBSN films. The first weight loss that occurred after 12 h can be attributed to the decomposition of the sulfonic acid groups in SPBSN matrix [9, 10]. The second weight loss that occurred after four days could stem from the decompositions of the main chain [15, 17]. The Nafion® 117 film has the best chemical stability. We expect that this occurred because the carbon–fluorine bonds (C-F bonds) of the Nafion® 117 matrix had stronger covalent bonds than the carbon–carbon bonds (C–C bonds) of the SPBSN matrixes [3–6]. Nevertheless, most of the SPBSN films did not dissolve in Fenton's reagent within 12 h at 80 °C.

TGA of the SPBSN Films

Figure 8 shows the thermal stability of the SPBSN films. As shown in this figure, three consecutive weight loss steps were observed for all SPBSN films. The first weight loss of all SPBSN films in the temperature range from approximately 100 to 300 °C is related to the decomposition of the unreacted monomers and to residual DMSO (organic solvent) evaporation [11, 12]. The second weight loss occurred between approximately 300 and 340 °C and can be ascribed to the decomposition of the sulfonated SS (SSS) parts in the SPBSN film matrix [15]. The third weight loss of all SPBSN films at approximately 350 °C is attributable to the decomposition of the SPBSN main chain [17, 19]. All cases show that the thermal stability of the SPBSN films decreased with an increase in the SS content within the SPBSN matrix. However, the corresponding thermal stability outcomes show a stable pattern. We consider that this occurred because the cross-linked network system played a role in restraining the collapse of the polymer chains within the SPBSN matrix. Moreover, these findings indicate that the –H groups were very well substituted at the phenyl side chains of the SS, within the raw-PBSN film via the pretreatment process.

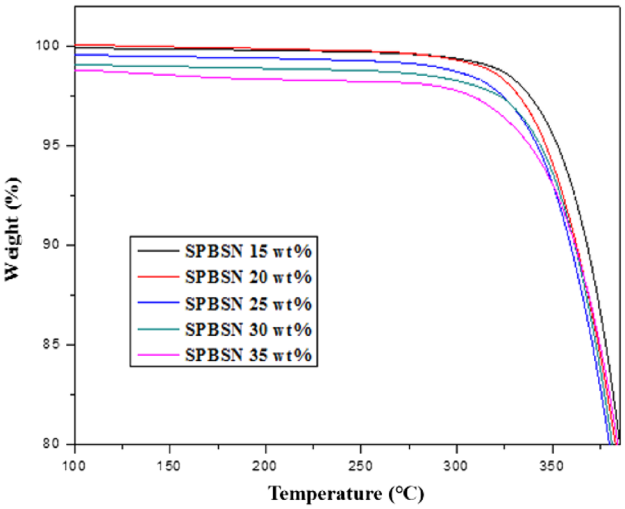

Fig. 8 Thermal stability of the SPBSN films

Swelling Ratio of the SPBSN Films

Figure 9 shows the SR of the Nafion® 117 and SPBSN films. As shown in this figure, the respective SR levels for the SPBSN 15 wt%, SPBSN 20 wt% and SPBSN 25 wt% films are approximately 42%, 76% and 107%, nearly 64%, 34% and 7% lower compared to that of Nafion® 117 (approximately 115%). The corresponding SR levels of the SPBSN 30 wt% and SPBSN 35 wt% films are approximately

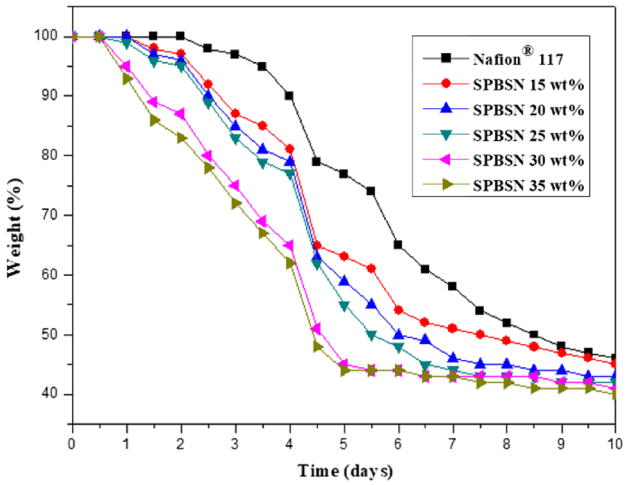

Fig. 7 Oxidative stability of the SPBSN films

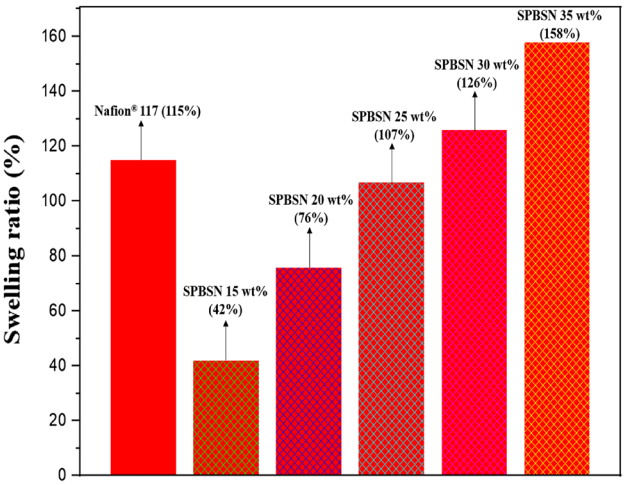

Fig. 9 Swelling ratios of the Nafion® 117 and SPBSN films

126% and 158%, close to 10% and 37% higher compared to that of Nafion® 117. All cases show that the SR level of the SPBSN films increased with an increase in the SS content within the SPBSN matrix. Because water in PEMs is absorbed only into their hydrophilic domains [25, 27], it can be concluded that the SS contents were increased within the SPBSN matrix. Even more interesting is that the SPBSN 35 wt% film retained its membrane form despite its very high level of SR. We consider that this occurred because the cross-linked network system played a role in preventing the absorption of water and restraining the expansion of the hydrophilic domains within the SPBSN 35 wt% film matrix [14, 15]. We also regard that the elastic chain of the BA that exists in the SPBSN 35 wt% film matrix underwent somewhat less morphological change due to the relaxation of the border between the hydrophilic domains and the hydrophobic domains [17, 18]. SPBSN films containing SS contents exceeding 40 wt% were easily torn and partially soluble in water, most likely because the cross-linked networks and elastic chains were collapsed by the excessive water within the SPBSN matrix.

Water Uptake of the SPBSN Films

Figure 10 shows the WU of the Nafion® 117 and SPBSN films. As shown in this figure, the respective WU levels for the SPBSN 15 wt%, SPBSN 20 wt% and SPBSN 25 wt% films are approximately 57%, 68% and 91%, nearly 53%, 44% and 26% lower compared to that of Nafion® 117 (approximately 123%). The corresponding WU levels of the SPBSN 30 wt% and SPBSN 35 wt% films are approximately 137% and 178%, close to 11% and 44% higher compared to that of Nafion® 117. In common with the SR outcomes, these findings indicate that the hydrophilic domains of the SPBSN films increased with an increase in the SS content within the SPBSN matrix [24, 25].

Ion Exchange Capacity of the SPBSN Films

Figure 11 shows the IEC values of the Nafion® 117 and SPBSN films. The IEC values for the SPBSN 15 wt% and SPBSN 20 wt% films are 1.61 meq/g and 1.70 meq/g, respectively, close to 9.0% and 3.9% lower compared to that of Nafion® 117 (approximately 1.77 meq/g). The corresponding IEC values of the SPBSN 25 wt%, SPBSN 30 wt% and SPBSN 35 wt% films are approximately 3.42 meq/g, 4.48 meq/g and 5.12 meq/g, close to 93.2%, 153.1% and 189.2% higher compared to that of the Nafion® 117 specimen. Like the SR pattern above, all cases show that the IEC value of the SPBSN films increased with an increase in the SS content within the SPBSN matrix. Because the IEC value is determined by the amount of H^+ released from the PEMs [5, 10], it can be considered that the SSS part as an ion-exchanger of H^+ was increased within the SPBSN matrix. It should be noted that the SPBSN 20 wt% film had a much lower SR level despite having an IEC value similar to that of Nafion® 117. We expect that this arose due to the cross-linked network system, which played a role in blocking the release of H^+ within the SPBSN 20 wt% film matrix [25, 27]. On the other hand, the SPBSN 25 wt%, SPBSN 30 wt% and SPBSN 35 wt% films had much higher IEC values (by approximately 101.1%, approximately 163.5% and approximately 201.1%, respectively) compared to that of the SPBSN 20 wt% film. This result most likely stemmed from the decreased cross-linking density and increased number of ion-exchangers that could release H^+ as the SS content was increased within the SPBSN matrix.

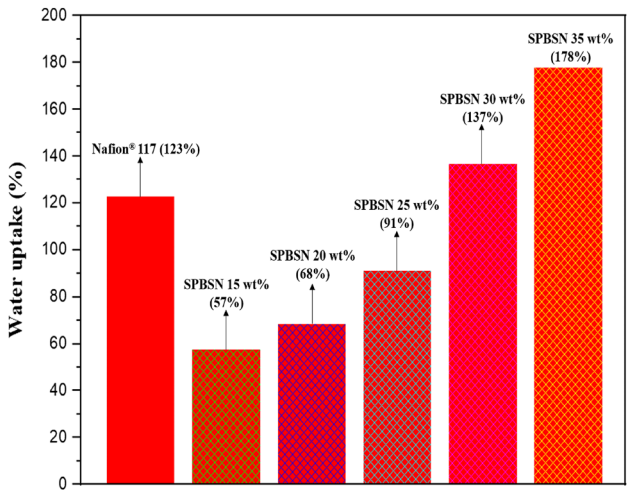

Fig. 10 Water uptake of the Nafion® 117 and SPBSN films

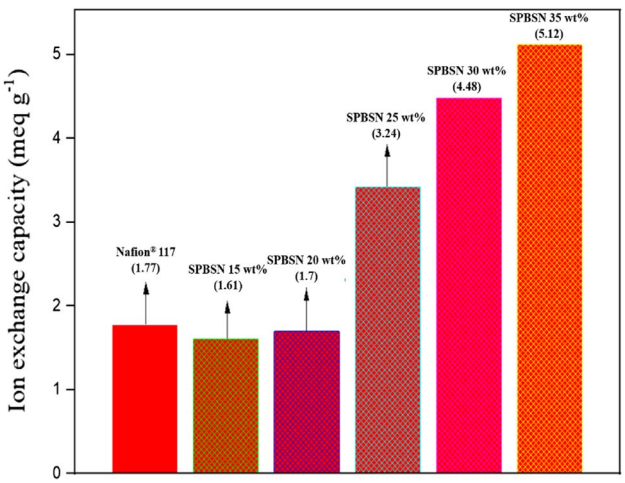

Fig. 11 Ion exchange capacities of the Nafion® 117 and SPBSN films

Proton Conductivity of the SPBSN Films

Figure 12 shows the PC outcomes of the Nafion® 117 and SPBSN films at various temperatures. At 50, 60, 70 and 80 °C, the PC values for the SPBSN 15 wt%, SPBSN 20 wt%, SPBSN 25 wt%, SPBSN 30 wt% and SPBSN 35 wt% films ranged from approximately 0.0017 S/cm to approximately 0.211 S/cm. Like the SR and IEC patterns above, all cases show that the PC values of the SPBSN films increased with a rise in the SS content within the SPBSN matrix and improved with an increase in the temperature. Because the PC value in PEMs is proportional to the concentration of H^+ [26, 27], it can be expected that the IEC value and H^+ mobility had both increased within the SPBSN matrix. However, the SPBSN films (SPBSN 15 wt% film, SPBSN 20 wt% film and SPBSN 25 wt% film) containing SS contents below 25 wt% had much lower PC values despite the fact they had similar or much higher IEC values compared to that of Nafion® 117 within the same temperature range. We consider that their poor SR obstructed the transportation of H^+ within the SPBSN matrixes [12, 14]. We also regard that the high cross-linking density of these specimens played a role in blocking the migration of H^+ [20, 23]. The SPBSN 30 wt% and SPBSN 35 wt% films had higher PC values compared to that of Nafion® 117 in the same temperature range. The SPBSN 35 wt% film had the best PC value. These results allow the clear conclusion that the rich SR level and high IEC value increased the activity of H^+ within the matrix as the cross-linking density was decreased as the SS content was increased within the SPBSN matrix.

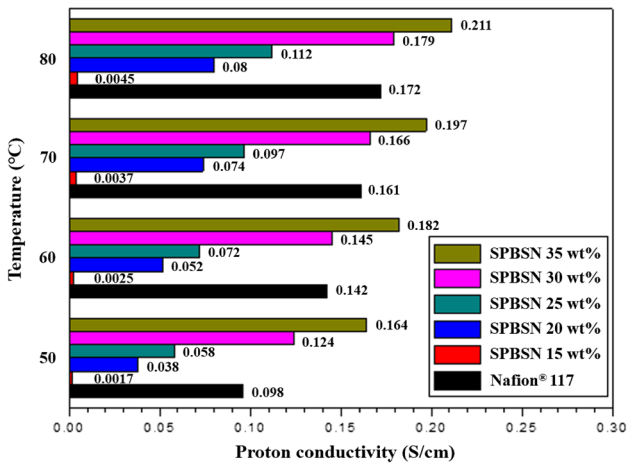

Fig. 12 Proton-conductivity levels of the Nafion® 117 and SPBSN films at various temperatures

Transmission Electron Microscope Image of the SPBSN Films

Figure 13 shows TEM images of the Nafion® 117 and SPBSN films, which were stained by a Pb^{2+} solution before the measurement. As shown in the figure, gray spots exist within the SPBSN matrix. Because Pb^{2+} ions are soluble in water [14, 15], it can be regarded that hydrophilic domains were displayed within the SPBSN matrix. Like the SR, IEC and PC patterns above, all cases show that the sizes and darkness levels of the hydrophilic domains were increased with an increase in the SS content within the SPBSN matrix. Judging from this, we believe that the SR, IEC and PC patterns of the SPBSN films depended on the hydrophilic domain sizes and darkness levels. The SPBSN 25 wt% film as an exception had a lower SR level and lower PC value, with a much higher IEC value despite its larger hydrophilic domain size and darker appearance compared to that of Nafion® 117. We consider that this result arose due to the unique characteristics of the sulfonated cross-linked films constituting the cross-linked networks [21, 22]. The size and darkness of the hydrophilic domains for the SPBSN 30 wt% and SPBSN 35 wt% films were drastically increased compared to those of the Nafion® 117 and other SPBSN films. The SPBSN 35 wt% film had the most obvious darkness and most extensive hydrophilic domains. As a result, the SR, IEC and PC of the SPBSN films were proportional to the hydrophilic domain sizes and darkness levels within the matrix. We could confirm that cross-linking polymerization was suitably performed through the TEM images of each SPBSN film with different contents of SS within the SPBSN matrix. Moreover, we were able to predict the SR, IEC and PC degrees for the SPBSN films through the TEM images.

Conclusions

In summary, SPBSN films were prepared via a pretreatment method after a curing process using various functional monomer mixtures. The SPBSN films as investigated here showed the formation of a high-quality styrene-based sulfonated cross-linked polymer membrane. All SR, IEC and PC patterns of these specimens improved with an increase in the SS content within the matrixes. In particular, the PC value, IEC value, SR level and WU level of the SPBSN 35 wt% film were approximately 0.211 S/cm, 5.12 meq/g, 158% and 178%, corresponding to increases of 22.6%, 189.2%, 37% and 44% relative to the same values for Nafion® 117 under identical conditions. These results arose due to the precise combination between the hard segments of NPGDA and the soft segments of BA within the SPBSN matrix.

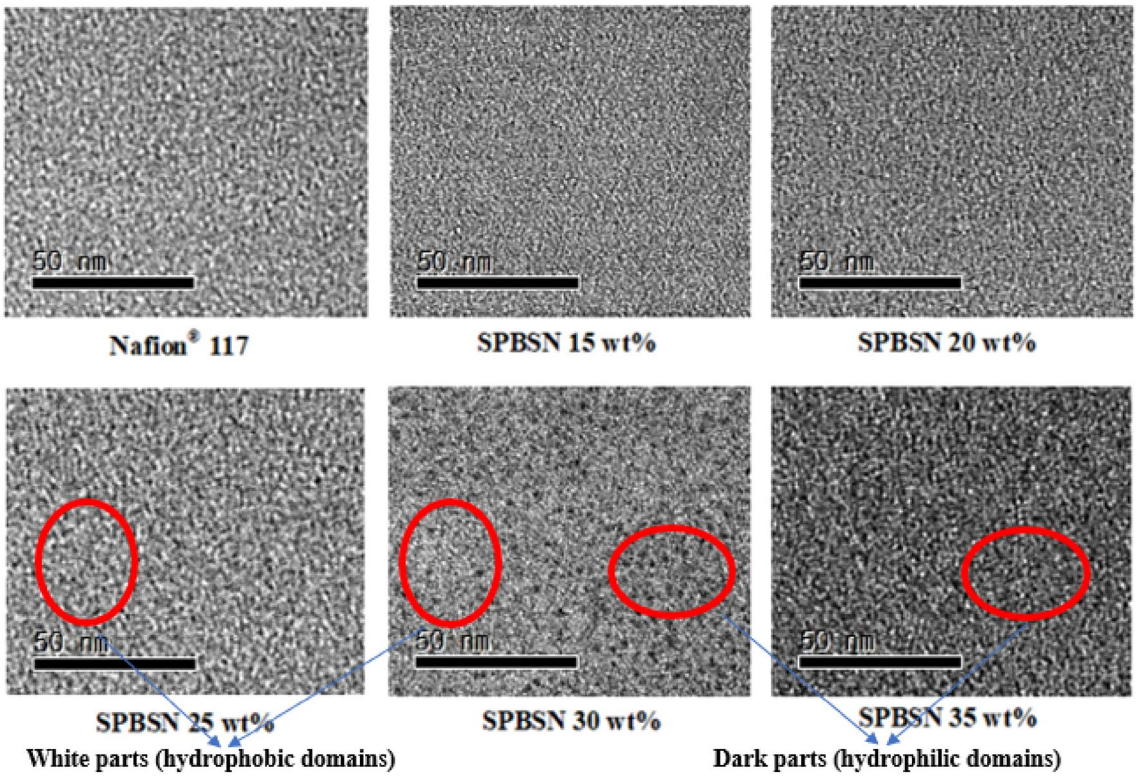

Fig. 13 TEM images of the Nafion® 117 and SPBSN films

Acknowledgements This work was supported by the Korea Institute of Energy Technology Evaluation and Planning (KETEP) grant funded by the Korea government (MOTIE) (20124000000090, Fostering human resources training in advanced hydrogen energy industry).

References

1. T. Jamal, G.M. Shafiullah, F. Dawood, A. Kaur, M.T. Arif, R. Pugazhendhi, R.M. Elavarasan, S.F. Ahmed, Energy Rep. **10**, 2103 (2023)
2. T. Higashihara, K. Matsumoto, M. Ueda, Polymer **50**, 5341 (2009)
3. F.S. Nanadegani, B. Sunden, Int. J. Hydrogen Energ. **48**, 32875 (2023)
4. A.R. Kim, M. Vinothkannan, D.J. Yoo, Int. J. Hydrogen Energ. **42**, 4349 (2017)
5. H. Bai, W.S.W. Ho, J. Taiwan Inst. Chem. Eng. **40**, 260 (2009)
6. S. Chen, X. Zhang, K. Chen, N. Endo, M. Higa, K.I. Okamoto, L. Wang, J. Power. Sources **196**, 9946 (2011)
7. G. Ito, M. Tanaka, H. Kawakami, Solid State Ion. **317**, 244 (2018)
8. W.J. Lee, H. Jung, K. Yang, Solid State Ion. **164**, 65 (2003)
9. S.Y. Jang, S.H. Han, J. Membr. Sci. **444**, 1 (2013)
10. C.C. Lin, C.B. Chang, Y.Z. Wang, J. Power. Sources **223**, 277 (2013)
11. K. Sato, T. Kajita, A. Noro, A.C.S. Appl, Polym. Mater. **5**, 3480 (2023)
12. H.X. Sun, Y.M. Fu, X. Meng, H.N. Wang, Y.O. He, R.G. Yang, Z.M. Su, Mater. Chem. Phys. **280**, 125845 (2022)
13. J.Y. Kim, S. Mulmi, C.H. Lee, H.B. Park, Y.S. Chung, Y.M. Lee, J. Membr. Sci. **283**, 172 (2006)
14. S.Y. Jang, S.H. Han, J. Nanosci. Nanotechnol. **19**, 1 (2019)
15. S.Y. Jang, S.H. Han, J. Ind. Eng. Chem. **23**, 285 (2015)
16. J. Lemus, A. Eguizabal, M.P. Pina, Int. J. Hydrogen Energ. **40**, 5415 (2015)
17. C. Charalampopoulos, K.J. Kallitsis, C. Anastasopoulos, M. Daletou, S.G. Neophytides, A.K. Andreopoulou, J.K. Kallitsis, Int. J. Hydrogen Energ. **45**, 35053 (2020)
18. S.U. Kim, D.M. Yu, T.H. Kim, Y.T. Hong, S.Y. Nam, J.H. Choi, J. Ind. Eng. Chem. **23**, 316 (2015)
19. S. Swaby, N. Urena, M.T. Perez-Prior, C. Rio, A. Varez, J.Y. Sanchez, C. Iojoju, B. Levenfeld, J. Ind. Eng. Chem. **122**, 366 (2023)
20. K. Oh, B. Son, J. Sanetuntikul, S. Shanmugam, J. Membr. Sci. **541**, 386 (2017)
21. K. Chen, Z. Hu, N. Endo, M. Higa, K.I. Okamoto, Polymer **52**, 2255 (2011)
22. C.X. Lin, Y.Z. Zhuo, E.N. Hu, Q.G. Zhang, A.M. Zhu, Q.L. Liu, J. Membr. Sci. **593**, 24 (2017)
23. G. Zeng, D. Zhang, L. Yan, B. Yue, T. Pan, Y. Hu, S. He, H. Zhao, J. Zhang, Int. J. Hydrogen Energ. **46**, 20664 (2021)
24. K. Fatyeyeva, J. Bigarre, B. Blondel, H. Galiano, D. Gaud, M. Lecardeur, F. Poncin-Epaillard, J. Membr. Sci. **266**, 33 (2011)
25. P. Salarizadeh, M. Javanbakht, S. Pourmahdian, M.S.A. Hazer, K. Hooshyari, M.B. Askari, Int. J. Hydrogen Energ. **44**, 3099 (2019)

26. F. Niepceron, B. Lafitte, H. Galiano, J. Bigarre, E. Nicol, J.F. Tassin, J. Membr. Sci. **338**, 100 (2009)
27. C.A. Dai, C.P. Liu, Y.H. Lee, C.J. Chang, C.Y. Chao, Y.Y. Cheng, J. Power. Sources **177**, 262 (2008)